Electrical Conduction Mechanism in Chemically Derived Graphene Monolayers

Alan B. Kaiser,[†] Cristina Gómez-Navarro,[‡,*] Ravi S. Sundaram,[‡] Marko Burghard,[‡] and Klaus Kern[‡,§]

MacDiarmid Institute for Advanced Materials and Nanotechnology, SCPS, Victoria University of Wellington, PO Box 600, Wellington, New Zealand, Max-Planck-Institut fuer Festkoerperforschung, Heisenbergstrasse 1, 70569 Stuttgart, Germany, and Ecole Polytechnique Federale de Lausanne, CH-1015 Lausanne, Switzerland

ABSTRACT

We have performed a detailed study of the intrinsic electrical conduction process in individual monolayers of chemically reduced graphene oxide down to a temperature of 2 K. The observed conductance can be consistently interpreted in the framework of two-dimensional variable-range hopping in parallel with electric-field-driven tunneling. The latter mechanism is found to dominate the electrical transport at very low temperatures and high electric fields. Our results are consistent with a model of highly conducting graphene regions interspersed with disordered regions, across which charge carrier hopping and tunneling are promoted by strong local electric fields.

Graphene, consisting of a layer of carbon atoms just one atom thick, is the ultimate in thin conducting sheets.[1] The charge carriers can be tuned from electron-like to hole-like by the application of a gate voltage,[2] and very high carrier mobilities have been reported.[3] Future electronics applications envisage the creation of diverse nanoscale elements of electronic circuits on a single graphene sheet.[1,4] However, progress in this direction is hampered by the limited availability of high-quality, large size graphene sheets. A promising solution to this problem comprises chemical conversion of readily accessible monolayers of graphene oxide (GO) to graphene.[5,6] To date, chemically derived graphene obtained in this manner exhibits an electrical conductivity of the order of a few Siemens per centimeter (approximately 3 orders of magnitude below that of pristine graphene layers[2,7]), which is useful for various applications such as transparent conducting electrodes[8] in photovoltaic cells[9−11] or electrically conductive composite materials.[12,13] The GO route is furthermore attractive since it may enable implementing electrically active graphene regions together with well-defined charge transport barriers made of GO into the same sheet.[14,15] However, at the present stage only little is known about the inherent microscopic structure and mechanism of electrical conduction, despite their great importance for the further improvement of this material. It is well-documented that GO-derived graphene contains a significant amount of residual defects,[6,16] and a detailed knowledge of how charge transport occurs in such a structurally and electronically inhomogeneous system could aid identifying synthetic strategies to more closely approach the electrical performance of pristine graphene.

Scanning tunneling microscopy (STM) of reduced GO monolayers has revealed that the hexagonal lattice of graphene sheets is partially preserved, but disordered regions ascribed to the presence of oxygenated functional groups are also present.[6] Moreover, the evaluation of Raman spectroscopic data on the basis of the empirical Tuinstra−Koenig expression[17] relating the intensity ratio of the Raman D and G modes to the crystallite size of graphitic samples provided an estimated size of the intact graphene regions on the order of 6 nm. Regarding the charge transport mechanism in GO-derived graphene, no conclusive picture has evolved so far.[18] In fact, while a previous study suggests the relevance of hopping conduction,[6] electrical measurements on overlapping platelets of reduced GO could be best interpreted in terms of tunneling through Schottky barriers at the gold contacts.[19] Similar to the latter case, the electrical resistance of GO flakes deposited between two epitaxial graphene electrodes has been found to be primarily due to Schottky barriers at the contacts.[20] As the current−voltage behavior showed no systematic dependence on the gap width between the electrodes, it was concluded that the dominant contribution

* Corresponding author, c.gomez-navarro@fkf.mpg.de.
† Victoria University of Wellington.
‡ Max-Planck-Institut fuer Festkoerperforschung.
§ Ecole Polytechnique Federale de Lausanne.

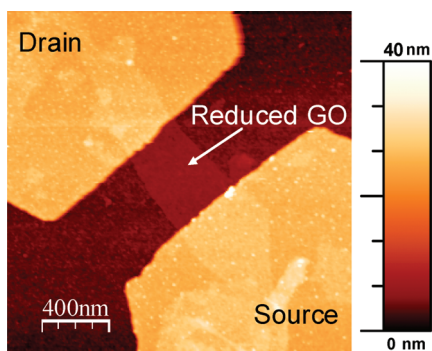**Figure 1.** An example of a reduced graphene oxide sample on a Si/SiO$_2$ substrate with Ti/AuPd (0.3/25 nm) top contacts.

to the measured resistance came from the contacts, and not the bulk resistance of the GO flake.

In this Letter, we report a detailed investigation of the intrinsic mechanisms of conduction in reduced GO monolayers. For our configuration and samples, the intrinsic resistance of the reduced GO sheets dominates over the graphene−electrode contact resistances. We measure and analyze currents as a function of electric field, gate voltage, and temperature down to 2 K. Our results on the conduction process in reduced GO sheets are relevant for the development of nanoscale devices comprised of patterned graphene sheets[14,15] and furthermore enable us to draw intriguing parallels to organic conducting polymers and carbon nanotubes, which display related structural features but a different dimensionality of their underlying π-systems.[21]

Graphite oxide prepared by the Hummers method[22] starting from graphite flakes was dispersed in water and deposited on a Si substrate with a 300 nm thick thermally grown SiO$_2$ layer that was previously surface-modified by aminosilanization. The resulting GO layers were chemically reduced by hydrogen plasma treatment, following an optimized procedure to obtain maximum electrical conductivity.[6] Individual GO monolayers, with atomic force microscope (AFM) heights of ∼1 nm, were provided with Ti/AuPd (0.3/ 25 nm) top contacts by e-beam lithography (Figure 1). For temperature-dependent electrical transport measurements, the samples were placed inside an Oxford Instrument cryostat under a low pressure of helium.

The investigation of GO monolayers contacted by a set of electrodes with varying distance revealed that their electrical resistance increases linearly with electrode separation (Figure 2a). This dependence shows that the total resistance of our samples is mainly governed by the intrinsic sheet resistance, rather than the contact resistance that in general should be independent of sample length. Further support for this conclusion stems from the fact that the temperature dependence of the measured source−drain current I does not fit well (Figure 2b) to the behavior

$$I(T) \propto T^{3/2} \exp(-1/T)$$

expected for Schottky barrier-limited charge transport.[20,23] The latter model has recently been successfully applied to
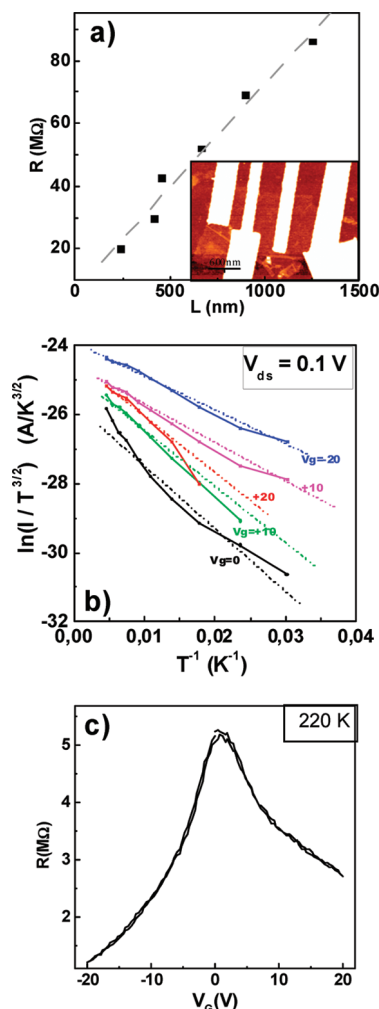

Figure 2. (a) Room-temperature resistance (measured at a voltage of ±100 mV) increasing linearly with electrode separation, illustrating that it arises primarily from the intrinsic resistance of the GO sheet rather than contact resistance at the electrodes. The inset shows the electrode configuration for the measurements. (b) Temperature dependence of the current I for a reduced GO sample (length 1.1 μm, width 1.3 μm), for a bias voltage of 0.1 V and different values of the gate voltage V_g (as shown), compared to the linear behavior (dashed lines) expected in this plot for the Schottky model. (c) Resistance as a function of gate voltage for the same sample as in panel b at 220 K under a low pressure of helium.

GO sheets subjected to mild thermal annealing instead of chemical reduction.[20] Besides a different chemical composition, the contact-dominated behavior observed in ref 20 may originate from the use of bottom gold electrodes for contacting the sheets, as distinguished from our noble metal contacts evaporated on top. In analogy to previous studies on carbon nanotubes,[24] such a configuration is expected to cause significant bending of the sheets at the electrode edges, which is likely to introduce a local potential barrier.

We are able to give an excellent account of our data down to a temperature of about 40 K in terms of variable-range hopping (VRH). In Figure 3, the current I measured between 2 and 200 K through a chemically reduced GO sheet at different gate voltages V_g from −20 to +20 V is compared for three different values of bias voltage V_{ds}. In each case, the current (and so conductance) is smallest for zero gate
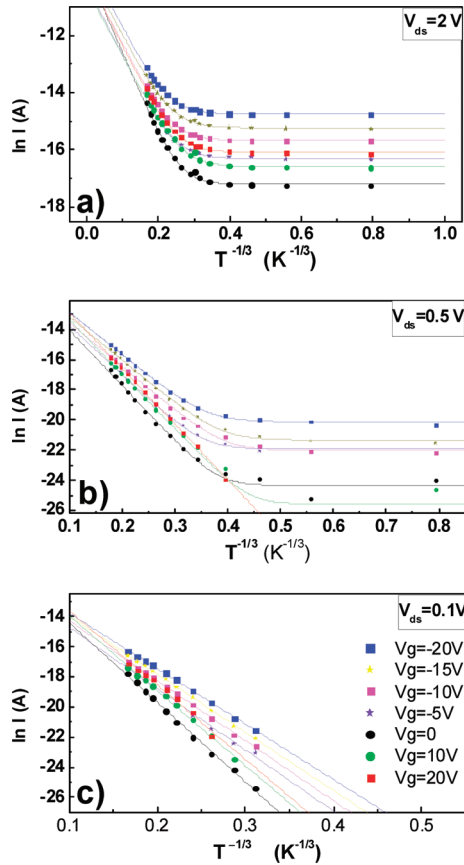
Figure 3. Natural logarithm of the measured current I vs $1/T^{1/3}$ fitted to eq 1 representing 2D variable-range hopping in parallel with a temperature-independent term, for different values of the gate voltage V_g as indicated, for bias voltages (a) $V_{ds} = 2$ V, (b) $V_{ds} = 0.5$ V, and (c) $V_{ds} = 0.1$ V.

voltage, at which the charge neutrality point was observed (see Figure 2c). All plots exhibit an asymmetry between the effect of positive and negative gate voltages, with negative V_g values producing a greater increase in conductance than corresponding positive values. A further common feature of the plots is that at higher temperatures the natural logarithm of the current shows a linear dependence on $T^{-1/3}$, which is indicative of two-dimensional (2D) VRH conduction.[25]

For the lowest value of bias voltage ($V_{ds} = 0.1$ V), all the measured data follow the 2D VRH law (from 216 K down to 34 K) (Figure 3c). At the higher bias voltage $V_{ds} = 0.5$ V, the currents are larger and the measured data extend down to lower temperature (Figure 3b). For this bias voltage, we find a deviation from the 2D VRH behavior for temperatures below ∼40 K, namely, a flattening of the temperature dependence as temperature decreases that occurs faster at negative gate voltages. For the largest bias voltage ($V_{ds} = 2$ V), for all values of gate voltage there is a clear flattening trend below ∼100 K, with essentially temperature-independent behavior below 25 K down to the limit of measurements at a temperature of 2 K (Figure 3a).

Further analysis shows that the overall temperature-dependent conductance ($G(T) = I/V_{ds}$) in Figure 3 is in excellent agreement with the expression

$$G(T) = G_1 \exp\left(-\frac{B}{T^{1/3}}\right) + G_0 \qquad (1)$$

where the first term represents the usual 2D VRH conduction expression[25] and the second term (discussed below) represents purely field-driven conduction without thermal activation, i.e., independent of temperature. The hopping parameter B depends on the density of states $N(E_F)$ near the Fermi level and the localization length L_l of the electronic wave functions involved; for 2D VRH the dependence is given by[25]

$$B = \left(\frac{3}{kN(E_F)L_l^2}\right)^{1/3} \qquad (2)$$

where k is Boltzmann's constant. The fitted values of this hopping parameter B (the magnitude of the slope of the linear portions at higher temperatures of the fits in Figure 3) are plotted in Figure 4a as a function of V_g for the three different bias voltages. It can be seen that in each case the value of B shows a peak when the gate voltage V_g is zero, reflecting the expected minimum in the graphene density of states (the interpretation in the case of high bias fields is complex as indicated below). At small bias voltages, there is an obvious asymmetry in the effect of applying the gate voltage. The application of a negative gate voltage significantly decreases the value of B, as would be expected for an increase in the hole density of states as the gate voltage shifts the Fermi level away from the charge neutrality point. However, the values of B for positive gate voltages are considerably larger than those for the corresponding negative gate voltages, indicating (according to eq 2) shorter localization lengths L_l and/or fewer electron carriers (which of course is consistent with the observed lower conductance for positive V_g). Very recently, the origin of electron−hole conduction asymmetry in graphene has been investigated and accounted for by pinning of charge density below metal electrodes[26] or by imbalanced carrier injection from graphene electrodes due to dopants.[27] However, in our samples, where the total resistance is dominated by the resistance of the reduced GO sheet rather than by electrode effects, it is more likely that the asymmetry is due to asymmetric scattering by charged impurities[28] that may be important in many graphene samples,[29] including our samples with more disorder. Greater scattering could reduce the mobility of electron carriers and decrease their localization lengths L_l relative to hole carriers. The values of the temperature-independent conductance term G_0 gained from the fits are shown in Figure 4b. No temperature-independent term is observed for the lowest bias ($V_{ds} = 0.1$ V) down to the limit of measurement (34 K). For bias voltage $V_{ds} = 0.5$ V, G_0 is observed but there is a strong decrease in G_0 as the gate voltage V_g increases from −20 V to positive values (above +10 V, the values are too difficult to measure). We suggest this trend as V_g is varied is also correlated with the asymmetry of scattering of electrons and holes, with the greater localization of electrons contributing to the suppression of the G_0 term at higher positive values of V_g.

For the highest bias voltage ($V_{ds} = 2$ V), G_0 is greatly increased by more than a factor of 50, as compared to the
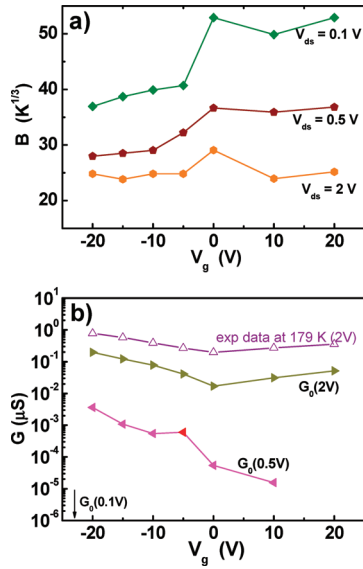
Figure 4. Parameters for the fits in Figure 3, plotted as a function of gate voltage V_g for different values of bias voltage V_{ds}. (a) Hopping parameter B. (b) Temperature-independent conductance G_0 (with bias voltage V_{ds} given in parentheses). Experimental values of conductance at a temperature of 179 K for $V_{ds} = 2$ V are also shown for comparison.

Figure 5. (a) Nonlinear $I-V$ characteristics and (b) conductance, G, plotted on a base 10 logarithmic scale as a function of bias voltage V_{ds} for different gate voltages V_g as indicated at a temperature of 220 K, for a chemically reduced graphene monolayer sample (channel length 1.1 μm, width 1.3 μm). The lines are fits to eq 3 for 2D VRH (the fit parameters are discussed in the text).

case of $V_{ds} = 0.5$ V. The values of G_0 for $V_{ds} = 2$ V show a variation with gate voltage that parallels that of the total experimental conductance at higher temperatures (the data for 179 K are included in Figure 4b), showing the minimum at the charge neutrality point and a similar (relatively small) electron–hole asymmetry. The behavior at high bias voltage is discussed further below in the context of our inhomogeneous conduction model.

In order to evaluate more specifically the dependence of VRH on bias voltages in our reduced GO monolayers, we have measured current–voltage ($I-V_{ds}$) characteristics up to $V_{bias} = \pm 2$ V at fixed temperatures. The data obtained at $T = 220$ K are plotted in Figure 5a. For VRH, the dependence of the conductance $G(T,E)$ on the bias electric field strength E (for small fields) is calculated[25,30] to be given by including a second multiplicative exponential term so that eq 1 becomes

$$G(T,E) - G_0 = G_1 \exp\left(-\frac{B}{T^{1/3}}\right) \exp\left(\frac{0.18er(T)}{kT}E\right) \quad (3)$$

where e is electronic charge and $r(T)$ is the mean low-field hopping distance that increases as temperature is lowered. On the basis of this equation, the conductance at fixed temperature is expected to initially increase exponentially with the strength of the applied field E or bias voltage V_{ds}, starting from its value $G(T,0)$ in the zero-field limit. Such an exponential increase with field E is indeed observed in the present samples at a temperature of 220 K, as demonstrated by Figure 5b where the conductance G at 220 K is plotted on a logarithmic scale versus bias voltage V_{ds}. The slope of the fitted lines in Figure 5b (averaged over positive and negative values of V_{ds}) is 0.238 V^{-1} for $V_g = 0$,
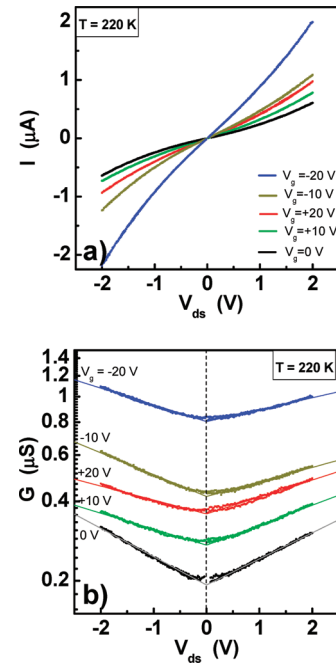
decreasing to 0.135 V^{-1} for $V_g = +20$ V, and to 0.125 V^{-1} for $V_g = -20$ V (note that this effect is comparable for positive and negative values of V_g, i.e., for electrons and holes). This trend of decreasing bias field effect with increasing magnitude of the gate voltage is expected from eq 3 since the hopping distance $r(T)$ decreases at the larger Fermi level density of states away from the neutrality point, thus further corroborating the validity of the VRH model to describe the charge transport in the reduced GO sheets.

However, a quantitative estimation of the hopping distances $r(T)$ provides evidence that VRH occurs only in part of the sample. If the bias electric field E producing the hopping were uniform across the sample, i.e., equal to the average field $E_{av} = V_{ds}/L$, where $L = 1.1$ μm is the separation of the electrodes, the hopping distances calculated from the experimental values of the slopes in Figure 5b would be $r(220$ K$) = 63$ nm for $V_g = 0$ and 33 nm for $V_g = -20$ V. These values are considerably larger than the size of 6 nm for the disordered regions and ordered graphene islands inferred from STM and Raman data on our samples,[6] which strongly suggests that an assumption of uniform field would be wrong. It is hence concluded that the actual fields in the hopping regions are an order of magnitude larger than the average field strength, leading to much shorter hopping distances. This implies the presence of relatively high conductance within the intact graphene "islands" that retain the hexagonal structure, with thin "barrier" regions representing a small fraction of the path across which most of the voltage drop occurs. We note that conduction will be dominated by paths with the thinnest barriers, and even a
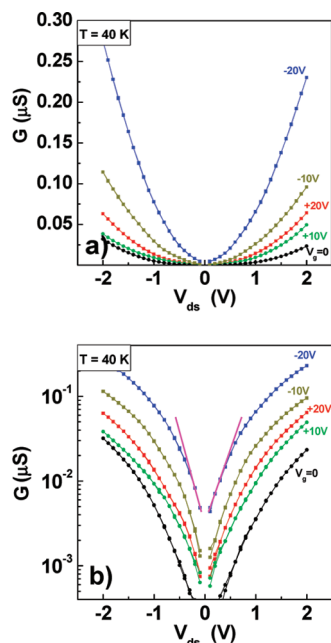
Figure 6. Conductance G plotted on a linear scale (a) and on a base 10 logarithmic scale (b) as a function of bias voltage V_{ds} for different gate voltages V_g as indicated, at a temperature of 40 K. The magenta lines represent the approximate linear slope of log G vs V_{ds} at lower values of V_{ds} for $V_g = -20$ V (see text for discussion). The lines joining the data points are guides for the eye.

narrow highly conducting path between ordered "islands" would short out hopping barrier regions and greatly reduce the fraction of path where conduction is by hopping.

This scenario is familiar from conduction in highly conducting polymers, which often consist of crystalline, metallic regions that are separated by disordered barriers that dominate the total resistance.[21] In the most highly conducting polymers such as doped polyacetylene, a large fraction of the conduction path is metallic, but the resistance is largely due to thin barriers (constituting only a few percent of the path) through which conduction is by fluctuation-assisted tunneling.[31] In this case, since tunneling can occur even in the zero temperature limit, an appreciable fraction of the conductance is retained as the temperature approaches zero. However, as the fraction of disordered polymer is increased, or the doping level reduced, there is an evolution to VRH conduction in larger disordered regions and the conductance decreases to zero in the zero-temperature limit (this latter case is analogous to the present 2D graphene sheets). An analogous behavior is also seen in single-wall carbon nanotube (SWCNT) networks, in which conduction is dominated by metallic tubes but is limited by conduction barriers formed by intertube contacts and defects along tubes.[32−34] As the thickness of the SWCNT networks is reduced, there is a change from fluctuation-assisted tunneling through thin barriers to 2D VRH through thicker barriers with conductivity extrapolating to zero in the zero-temperature limit.[32] The greater effect of disorder in 2D compared to 3D supports our proposed scenario for the reduced GO monolayers. Note that metallic-like conduction in ordered regions (essentially in series with the hopping conduction in barriers) would contribute a much smaller resistance than

the hopping and thus not significantly affect the temperature dependence of the total resistance, which at high temperatures remains characteristic of VRH.

At the lower temperature of 40 K, the corresponding plots of conductance G versus bias voltage V_{ds} in Figure 6 show a much stronger dependence on the electric field, as expected from eq 3 for 2D VRH upon decreasing temperature. The slope of the straight lines drawn in Figure 6b showing a typical data trend at low bias voltage V_{ds} is much larger than the average slope at 220 K (Figure 5a), as expected from the exponent in eq 3 at lower temperatures. However, it is apparent that the increase of $\log_{10} G$ with V_{ds} is no longer linear so at this lower temperature the field E used is too strong for eq 3 to be valid. Calculations of hopping as the field becomes large do predict a trend to saturation in the increase of $\log_{10} G$ with V_{ds}, and this effect has been documented for germanium films at lower temperatures.[25] On this basis, the observed decrease of G below the exponential increase as V_{ds} increases is in qualitative agreement with the expected trend for VRH.

Regarding the electrical behavior of the sheets at even lower temperatures, it is clear from extrapolating the high-temperature 2D VRH current in Figure 3 to 2 K that the magnitude of this term would be below our measurement limit (except possibly at the highest bias voltage). This reduction of the VRH conductance is associated with the longer hopping distances required as the Fermi window (width $\sim kT$) becomes small at low temperatures. In materials with a uniform density of localized states, field-driven hopping down the potential gradient without thermal activation (but with emission of phonons) is expected to become the conduction mechanism at very high fields.[25,30,35] This process yields a temperature-independent conductance, which will be most evident at low temperatures where thermally assisted hopping is frozen out and which may well contribute to the temperature-independent conduction term G_0 that we observe in parts a and b of Figure 3 at very low temperature.

However, we showed above that VRH hopping occurs only over part of the conduction paths (the disordered barrier regions separating highly conducting graphene islands), so we expect a parallel contribution to conductance from direct tunneling through the barriers between delocalized electron states in the well-ordered graphene regions. This is analogous to the process that gives the relatively large conductance in the zero-temperature limit often observed in highly conducting polymers and SWCNT networks.[21,32] The contribution in the reduced GO case would be smaller due to the greater thickness of the barrier regions, which also explains why hopping produces the increase in conductance at higher temperatures rather than fluctuation-assisted tunneling in the case of most highly conducting polymers.

As shown in Figure 4b, there is a dramatic increase in the temperature-independent conduction term G_0 at negative gate voltages V_g when the bias voltage is raised from $V_{ds} = 0.1$ to 0.5 V, and again at all V_g values at $V_{ds} = 2$ V (where the electron−hole asymmetry is greatly reduced). We cannot understand this conduction term seen below 10 K as an enhancement of the usual temperature-dependent VRH

conduction by the larger electric field as eq 3 successfully predicted at 220 K. Instead, the lack of temperature dependence of our samples below 10 K (parts a and b of Figure 3) shows that new purely field-driven conduction mechanisms are being initiated as V_{ds} increases, namely, direct tunneling (that requires no thermal excitation) through disordered barriers between delocalized electron states in the graphene islands (where these barriers are thin) and field-driven hopping through thicker barriers.

The fact that at $V_{ds} = 2$ V there is significant increase in the field-driven conduction at 2 K (Figure 3a) indicates that this bias voltage yields a potential drop across disordered barrier regions in the heterogeneous structure of the sheets that is a significant fraction of the typical barrier energy. This enables us to estimate the order of magnitude of the minimum barrier energy involved. The spacing of the barriers must be larger than the size of the intact graphene islands (∼6 nm), and could be considerably larger if some barriers are short-circuited by highly conducting paths as discussed above. So we take the separation of barrier centers as of order 7 ∼20 nm, and assuming the voltage drop across the highly conducting intact graphene islands is small, the typical voltage drop across the barriers would be of order 13−36 mV for a voltage of 2 V across the electrodes. Thus the minimum tunneling barrier energies involved might be on the order of 40 meV. The thermal energy kT at a temperature of 10 K is only ∼0.9 meV, confirming that thermally assisted conduction across such barriers would be expected to be very small below 10 K (as we find experimentally).

In summary, we have shown that the intrinsic conductance of chemically reduced graphene oxide sheets is in excellent agreement with a model of 2D VRH in parallel with field-driven tunneling. At higher temperatures, both the temperature- and electric field-dependence of conductance follow the behavior predicted for 2D VRH. The deduced values of the mean hopping distance point toward the presence of regions of delocalized states and relatively high conductance that are separated by disordered regions with localized states where the conduction is by hopping, a heterogeneous scenario that is consistent with the pattern of disordered regions interspersed with well-ordered graphene islands inferred from Raman and microscopic data.[6] The temperature-independent conductance remaining at low temperatures can be ascribed to tunneling between regions with delocalized states and field-driven hopping in the barriers.

References

(1) Geim, A. K.; Novoselov, K. S. *Nat. Mater.* **2007**, *6* (3), 183–191.
(2) Novoselov, K. S.; Geim, A. K.; Morozov, S. V.; Jiang, D.; Zhang, Y.; Dubonos, S. V.; Grigorieva, I. V.; Firsov, A. A. *Science* **2004**, *306* (5696), 666–669.
(3) Chen, J. H.; Jang, C.; Xiao, S. D.; Ishigami, M.; Fuhrer, M. S. *Nat. Nanotechnol.* **2008**, *3* (4), 206–209.
(4) Berger, C.; Song, Z. M.; Li, T. B.; Li, X. B.; Ogbazghi, A. Y.; Feng, R.; Dai, Z. T.; Marchenkov, A. N.; Conrad, E. H.; First, P. N.; de Heer, W. A. *J. Phys. Chem. B* **2004**, *108* (52), 19912–19916.
(5) Stankovich, S.; Piner, R. D.; Chen, X. Q.; Wu, N. Q.; Nguyen, S. T.; Ruoff, R. S. *J. Mater. Chem.* **2006**, *16* (2), 155–158.
(6) Gomez-Navarro, C.; Weitz, R. T.; Bittner, A. M.; Scolari, M.; Mews, A.; Burghard, M.; Kern, K. *Nano Lett.* **2007**, *7* (11), 3499–3503.
(7) Berger, C.; Song, Z. M.; Li, X. B.; Wu, X. S.; Brown, N.; Naud, C.; Mayo, D.; Li, T. B.; Hass, J.; Marchenkov, A. N.; Conrad, E. H.; First, P. N.; de Heer, W. A. *Science* **2006**, *312* (5777), 1191–1196.
(8) Blake, P.; Brimicombe, P. D.; Nair, R. R.; Booth, T. J.; Jiang, D.; Schedin, F.; Ponomarenko, L. A.; Morozov, S. V.; Gleeson, H. F.; Hill, E. W.; Geim, A. K.; Novoselov, K. S. *Nano Lett.* **2008**, *8* (6), 1704–1708.
(9) Eda, G.; Fanchini, G.; Chhowalla, M. *Nat. Nanotechnol.* **2008**, *3* (5), 270–274.
(10) Li, D.; Muller, M. B.; Gilje, S.; Kaner, R. B.; Wallace, G. G. *Nat. Nanotechnol.* **2008**, *3* (2), 101–105.
(11) Wang, X.; Zhi, L. J.; Mullen, K. *Nano Lett.* **2008**, *8* (1), 323–327.
(12) Stankovich, S.; Dikin, D. A.; Dommett, G. H. B.; Kohlhaas, K. M.; Zimney, E. J.; Stach, E. A.; Piner, R. D.; Nguyen, S. T.; Ruoff, R. S. *Nature (London)* **2006**, *442* (7100), 282–286.
(13) Watcharotone, S.; A, D. D.; Stankovich, S.; P., R.; Jung, I.; Dommett, G. H.B.; E, G.; W., S.-E.; C., S.-F.; L., C.-P.; N., S. T.; S., R. R. *Nano Lett.* **2007**, *7* (7), 1888–1892.
(14) Weng, L. S.; Zhang, L. Y.; Chen, Y. P.; Rokhinson, L. P. *Appl. Phys. Lett.* **2008**, *93* (9), xx.
(15) Giesbers, A. J. M.; Zeitler, U.; Neubeck, S.; Freitag, F.; Novoselov, K. S.; Maan, J. C. *Solid State Commun.* **2008**, *147* (9−10), 366–369.
(16) Stankovich, S.; Dikin, D. A.; Piner, R. D.; Kohlhaas, K. A.; Kleinhammes, A.; Jia, Y.; Wu, Y.; Nguyen, S. T.; Ruoff, R. S. *Carbon* **2007**, *45* (7), 1558–1565.
(17) Tuinstra, F.; Koenig, J. L. *J. Chem. Phys.* **1970**, *53* (3), 1126–&.
(18) Jung, I.; Dikin, D. A.; Piner, R. D.; Ruoff, R. S. *Nano Lett.* **2008**, *8*, 4283–4287.
(19) Gilje, S.; Han, S.; Minsheng, W.; Kang, L. W.; Kaner, R. B. *Nano Lett.* **2007**, *7* (11), 3394–3398.
(20) Wu, X. S.; Sprinkle, M.; Li, X.; Fan, M.; Berger, C.; De Heer, W. A. *Phys. Rev. Lett.* **2008**, *101*, 026801.
(21) Kaiser, A. B. *Adv. Mater.* **2001**, *13* (12−13), 927–939.
(22) Hummers, W. S.; Offeman, R. E. *J. Am. Chem. Soc.* **1958**, *80* (6), 1339–1339.
(23) Anwar, A.; Nabet, B.; Culp, J.; Castro, F. *J. Appl. Phys.* **1999**, *85* (5), 2663–2666.
(24) Bockrath, M.; Cobden, D. H.; Lu, J.; Rinzler, A. G.; Smalley, R. E.; Balents, T.; McEuen, P. L. *Nature (London)* **1999**, *397* (6720), 598–601.
(25) Mott, N. F.; A. Davis, E. *Electronic Processes in Non-Crystalline Materials*, 2nd ed.; Oxford University Press: Oxford, England, 1979.
(26) Huard, B.; Stander, N.; Sulpizio, J. A.; Goldhaber-Gordon, D. *Phys. Rev. B* **2008**, *78* (12), xx.
(27) Farmer, D. B.; Golizadeh-Mojarad, R.; Perebeinos, V.; Lin, Y. M.; Tulevski, G. S.; Tsang, J. C.; Avouris, P. *Nano Lett.* **2009**, *9* (1), 388–392.
(28) Novikov, D. S. *Appl. Phys. Lett.* **2007**, *91* (10), xx.
(29) Chen, J. H.; Jang, C.; Adam, S.; Fuhrer, M. S.; Williams, E. D.; Ishigami, M. *Nat. Phys.* **2008**, *4* (5), 377–381.
(30) Pollak, M.; Riess, I. *J. Phys. C: Solid State Phys.* **1976**, *9* (12), 2339–2352.
(31) Sheng, P. *Phys. Rev. B* **1980**, *21* (6), 2180–2195.
(32) Skakalova, V.; Kaiser, A. B.; Woo, Y. S.; Roth, S. *Phys. Rev. B* **2006**, *74* (8), xx.
(33) Kaiser, A. B. *Rep. Prog. Phys.* **2001**, *64* (1), 1–49.
(34) Gruner, G. *J. Mater. Chem.* **2006**, *16* (35), 3533–3539.
(35) Shklovskii, B. I. *Sov. Phys. Semiconduct.* **1973**, *6* (12), 1964–1967.

NL803698B